2016 IEEE 36th International Conference on Distributed Computing Systems

Energy Minimization for Quality-Constrained Video with Multipath TCP over Heterogeneous Wireless Networks

Jiyan Wu, Bo Cheng, Ming Wang
State Key Laboratory of Networking and Switching Technology,
Beijing University of Posts and Telecommunications, Beijing 100876, P. R. China.
Email: {wujiyan, chengbo, wangming_bupt}@bupt.edu.cn.

***Abstract*—The advancements in wireless infrastructures and communication technologies prompt the bandwidth aggregation for mobile video delivery over heterogeneous access networks. Multipath TCP (MPTCP) is the transport protocol recommended by IETF to enable concurrent data transmissions over multiple communication paths. However, it still remains problematic to deliver user-satisfied video services with the existing MPTCP schemes due to the contradiction between mobile device energy and video distortion. To enable the energy-efficient and quality-guaranteed video streaming, this paper presents an Energy-Distortion Aware MPTCP (EDAM) solution. First, we develop an analytical model to capture the energy-distortion tradeoff for multipath video transmission over heterogeneous wireless networks. Second, we propose a video flow rate allocation algorithm to minimize the energy consumption while achieving target video quality based on utility maximization theory. The performance of the proposed EDAM is evaluated through extensive emulations in Exata involving real-time H.264 video streaming. Evaluation results demonstrate that EDAM outperforms the reference MPTCP schemes in reducing energy consumption, as well as in improving video PSNR (Peak Signal-to-Noise Ratio).**

I. Introduction

The radical evolutions in wireless infrastructures provide mobile users with ubiquitous access options to the Internet, *e.g.*, cellular networks (UMTS, HSDPA, LTE), wireless local area networks (802.11 family), and broadband wireless networks (LTE, WiMAX). Supported by the latest technological progress, mobile terminals are equipped with multiple radio interfaces and enabled simultaneous access to different wireless networks (*e.g.*, the Samsung S5 smart phones can establish associations with both LTE and Wi-Fi networks using the Download Booster [1]). With the prevalence of such multihomed terminals, the future wireless environment is expected to be a converged system that incorporates heterogeneous access networks to provide high-quality mobile services [2].

Accelerated by the remarkable advancements in wireless communication systems, mobile video traffic has undergone exponential growth over the past few years. According to the latest Cisco report [3], video streaming accounts for 55% of the mobile data usage over the Internet in 2014 and will reach 72% by the year 2019. As the throughput demand of high-quality video streaming outpaces the available capacity in single wireless networks, new research trends have moved towards integrating the heterogeneous access medium for concurrent data transmissions [4-6]. However, the radio communication modules (*e.g.*, using Wi-Fi, 3G, and LTE) constitute a large portion of energy consumption in smart phones [7][8]. Current mobile devices are usually powered by batteries with limited capacities. Therefore, it is important to study the relationship between energy consumption and media quality to sustain multihomed video transmission over heterogeneous wireless networks [9].

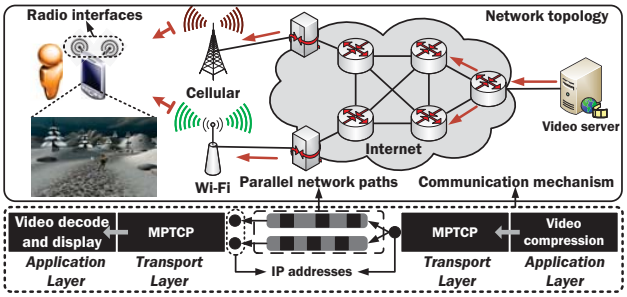

Fig. 1. Multihomed video communication with Multipath TCP (MPTCP) over heterogeneous wireless networks.

Multipath TCP (MPTCP) is the standard transport-layer protocol recommended by IETF (Internet Engineering Task Force) to enable parallel data transfer over communication networks with multihomed terminals (see Figure 1) [10-12]. However, it still remains problematic to deliver user-satisfied video service with the existing MPTCP schemes [4][10][24][27] *because there is an inherent tradeoff between the energy consumption and video quality* (Proposition 1 in Section II.C). In this paper, we address the critical problem by modeling and leveraging the energy-distortion tradeoff to optimize multihomed video communication with MPTCP over heterogeneous wireless networks. The proposed Energy-Distortion Aware MPTCP (EDAM) is able to effectively integrate the available resources in heterogeneous networks to minimize energy consumption under video quality constraint.

Specifically, the contributions of this study can be summarized in the following.

- Develop an analytical framework to model the relationship between end-to-end distortion and energy consumption for concurrent video transmission over multiple wireless access networks.
- Propose a flow rate allocation algorithm in MPTCP to

This research is supported by the National Natural Science Foundation of China (NSFC) under Grant No. 61132001; National High-tech R&D Program of China (863 Program) under Grant No. 2013AA102301; Program for New Century Excellent Talents in University under Grant No. NCET-11-0592.

1063-6927/16 $31.00 © 2016 IEEE
DOI 10.1109/ICDCS.2016.25

minimize the energy consumption under video quality constraint based on utility maximization theory and piecewise linear approximation.

- Perform extensive emulations in Exata involving H.264 video streaming. Evaluation results show that:
  1) EDAM reduces the energy consumption by up to 65.8 (26.3%) and 115.3 (40.6%) J (Joule) compared to the EMTCP [4] and MPTCP [10] while achieving the same video quality in 200 seconds.
  2) EDAM improves the PSNR by up to 7.3 (25.5%) and 10.3 (39.3%) dB compared to the EMTCP and MPTCP with the same energy consumption.
  3) EDAM increases the number of effective retransmissions by up to 22.3 (46.3%) and 36.7 (58.2%) compared to the EMTCP and MPTCP, respectively.

To the best of our knowledge, the proposed EDAM is the first MPTCP scheme that takes advantage of the energy-distortion tradeoff for multihomed video communication over heterogeneous wireless networks.

The remainder of this paper is structured as follows. In Section II, we present the system model to capture the energy-distortion tradeoff. Section III introduces the solution procedure of the proposed EDAM in detail. The performance evaluation is provided in Section IV and Section V gives the concluding remarks of this work.

II. System and Model Description

A. System Overview

The system overview of the proposed EDAM is presented in Figure 2. We consider the end-to-end transmission of a single video flow using the MPTCP connection over multiple wireless access networks. The goal of the proposed EDAM scheme is to minimize the energy consumption while achieving the target video quality (in terms of PSNR or distortion). The input video flow is divided into multiple sub-flows onto the available communication paths. Each sub-flow consists of several segments. The working components in the system design are implemented at both transmission ends and the key contribution of EDAM is in the flow rate allocation. In the sender side, the decision making blocks include the parameter control unit, flow rate allocator, and retransmission controller.

At the receiver side, the information feedback unit is responsible for sending back the channel status and acknowledgements (ACKs) at sub-flow level. The connection-level identification and ACK are specified in [10]. Due to the path asymmetry in heterogeneous wireless networks, the packets may arrive at the destination out-of-order. These packets will be reordered to restore the original video traffic. To mitigate the packet drop problem, the frame-copy error concealment is implemented at the receiver side.

The critical step in the energy and quality optimization is the *flow rate allocation* (*i.e.*, video data allocation over the available access networks). This problem involves the mathematical models of wireless access network, video distortion and energy consumption.

B. Model Description

Wireless Access Network Model

In the system model, we consider a heterogeneous wireless environment integrating P access networks between communication terminals. The end-to-end connection represents a communication path in MPTCP and can be constructed by binding a pair of IP addresses. With regard to the limited capacity and time-varying channel status, the wireless access link is most likely to be the bottleneck for end-to-end video transmission. Each communication path $p \in \mathcal{P}$ is considered to be an independent transport link uncorrelated with others and is characterized by the following properties.

- The available bandwidth μ_p, which denotes the time-varying share of that bandwidth as perceived by the end-to-end video flow.
- The round trip time RTT_p, which represents the duration it takes for a data packet to be sent plus the delay it takes for an acknowledgment of that packet to be received at the sender side.
- The packet loss rate π_p^B, which indicates the average loss probability of the packets dispatched onto communication path p.

In addition to the above metrics, we model burst loss on each path using the Gilbert loss model [13], which can be expressed as a two-state stationary continuous time Markov chain. The state $\mathcal{X}_p(t)$ at time t assumes one of two values: G (Good) or B (Bad). We assume the packet loss rate to be zero in the 'Good' state. If a packet is sent at time t and $\mathcal{X}_p(t) = G$ then the packet can be successful delivered. Conversely, if $\mathcal{X}_p(t) = B$ then the packet is lost. We denote by π_p^G and π_p^B the stationary probabilities that path p is good or bad. Let ξ_p^G and ξ_p^B represent the transition probability from B to G and G to B, respectively. In this work, we adopt two system-dependent parameters to specify the continuous time Markov chain packet loss model: (1) the channel loss rate π_p^B, and (2) the average loss burst length $1/\xi_p^B$. Then, we will have $\pi_p^G = \xi_p^G/(\xi_p^B + \xi_p^G)$ and $\pi_p^B = \xi_p^B/(\xi_p^B + \xi_p^G)$.

Video Distortion Model

To optimize the real-time streaming video quality, we employ a generic end-to-end video distortion model [14]. The user-perceived quality in video streaming environment is impacted by the the end-to-end distortion (D). Specifically, D is the sum of two major categories of distortion: source distortion (D_{src}) and channel distortion (D_{chl}), *i.e.*,

$$\mathsf{D} = \mathsf{D}_{\text{src}} + \mathsf{D}_{\text{chl}}. \tag{1}$$

This analytic model indicates the streaming video quality depends on both the distortion caused by the data compression of the media information and the distortion due to the transmission impairments in the communication network. The source distortion is mostly driven by the video encoding rate (R) and the video sequence content. These parameters largely impact the efficiency of video codec (*e.g.*, the larger distortion will be induced for a more complex video sequence under the same video encoding rate). The channel distortion is mainly impacted by the *effective loss rate* (Π) defined as follows.

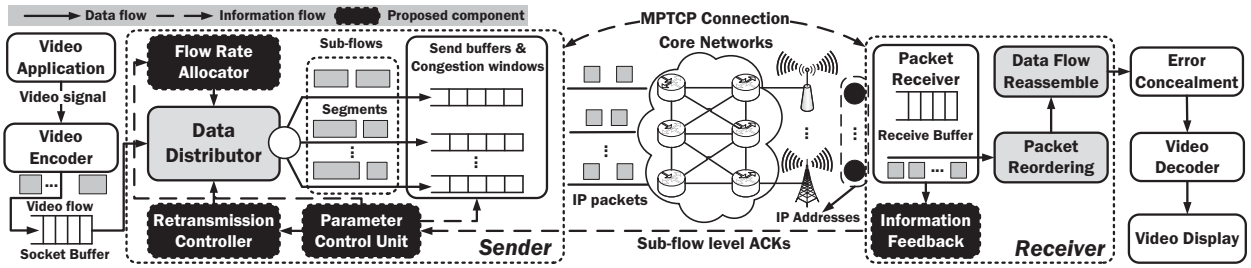

Fig. 2. System overview of the proposed EDAM (Energy-Distortion Aware MPTCP).

***Definition** 1:* The **effective loss rate** (Π) is the combined probability of both the channel errors/losses and expired packet arrivals.

D_{chl} is roughly proportional to the number of video frames that cannot be decoded. In particular, the end-to-end distortion can be expressed (in units of Mean Square Error, MSE) with the following equation [14]:

$$\mathsf{D} = \frac{\alpha}{R - R_0} + \beta \cdot \Pi, \tag{2}$$

in which α, R_0 and β are parameters depending on specific video codec and sequence. These parameters can be online estimated by using trial encodings at the sender side [14]. To allow fast adaptation of the transmission scheduling to abrupt changes in the video content, these parameters can be updated for each group of pictures (GoP).

Energy Consumption Model

We employ the e-Aware model [15] to characterize the energy consumption of mobile devices. This model considers the ramp, transfer and tail energy. The device-specific energy and power consumptions are profiled [in units of Joule (J) and Watt (W)] with the input parameters of signaling frequency, packet size and data transfers. In this work, we consider the media transfer as it constitutes the majority of energy consumption for multimedia streaming to mobiles [8]. The energy consumption parameter e_p for a specific communication path p is defined as the consumed energy for delivering the same amount of data traffic (J/Kbps). Then, the total energy consumption for the given rate allocation vector $\mathsf{R} = \{R_p\}_{p \in P}$ across all the paths can be expressed as

$$\mathbf{E} = \sum_{p \in P} R_p \cdot \mathsf{e}_p. \tag{3}$$

Extensive measurement studies reveal [8][15] that the energy consumed for transmitting the same amount of data through Wi-Fi network is lower than that across 3G (*e.g.*, WCDMA) and LTE.

Effective Loss Rate

The effective loss rate represents the combined probability of transmission and overdue data losses across all the communication paths. Therefore, the effective loss rate over p can be obtained with the following equation

$$\Pi_p = \pi_p^{\text{t}} + \left(1 - \pi_p^{\text{t}}\right) \cdot \pi_p^{\text{o}}, \tag{4}$$

in which π_p^{t} denotes the transmission loss rate and π_p^{o} represents the overdue loss rate. These terminologies are defined as follows.

***Definition** 2:* The transmission loss rate denotes the ratio of lost packets while traversing the communication network. These packet drops can be caused by the network congestion, channel fading, buffer overflow, etc.

***Definition** 3:* The overdue loss rate represents the probability of packets arriving at the destination out of the deadline (T) imposed by the video application.

First, we provide derivations of π_p^t based on continuous time Markov chain and Gilbert loss model.

In the scheduling process of MPTCP, the encoded video data (*e.g.*, a Group of Pictures with the total size S) is divided into multiple sub-flows ($S_p = (R_p \cdot S)/R, p \in \mathcal{P}$) and each of them is dispatched onto a different path. The segments will be fragmented into IP packets when transmitted over each communication path. Therefore, the number of packets on each path can be estimated with $n_p = \lceil S_p/MTU \rceil$, in which $\lceil x \rceil$ represents the smallest integer larger than x and MTU denotes the Maximum Transmission Unit size. We assume the packets over each path are evenly spread with interval ω_p. Let c denote a n-tuple that represents a specific path failure configurations. If the ith packet dispatched onto path p is lost, then $c_p^i = B, p \in \mathcal{P}, 1 \leq i \leq n_p$ and vice versa. By taking into account all the possible configurations of c_p, we can obtain the transmission loss rate π_p^{t} as

$$\pi_p^{\text{t}} = \frac{1}{n_p} \cdot \sum_{\text{all } c_p} L(c_p) \cdot \mathbb{P}(c_p), \tag{5}$$

in which "all c_p" denotes all the possible combinations of c_p and $L(c_p)$ represents the number of lost packets on path p. $L(c_p)$ can be expressed as

$$L(c_p) = \sum_{i=1}^{n_p} 1_{\{c_p^i = B\}}.$$

Suppose $\mathbb{P}(c_p^i)$ denotes the probability of path failure on p when delivering the ith packet. We can derive $\mathbb{P}(c_p^i)$ based on continuous time Markov chain and Gilbert loss model. Let $\mathsf{F}_p^{\langle i,j \rangle}(\omega_p)$ denote the probability of transition from state i to j on path p in time ω_p

$$\mathsf{F}_p^{\langle i,j \rangle}(\omega_p) = \mathbb{P}[\mathcal{X}_p(\omega_p) = j | \mathcal{X}_p(0) = i].$$

According to the transient behaviour of continuous time Markov chain, the state transition matrix can be expressed

as follows

$$\mathsf{F}_p^{\langle G,G\rangle}(\omega_p) = \pi_p^G + \pi_p^B \cdot \kappa_p,\ \mathsf{F}_p^{\langle G,B\rangle}(\omega_p) = \pi_p^B - \pi_p^B \cdot \kappa_p,$$
$$\mathsf{F}_p^{\langle B,G\rangle}(\omega_p) = \pi_p^G - \pi_p^G \cdot \kappa_p,\ \mathsf{F}_p^{\langle B,B\rangle}(\omega_p) = \pi_p^B + \pi_p^G \cdot \kappa_p,$$

where $\kappa_p = \exp\left[-\left(\xi_p^B + \xi_p^G\right) \cdot \omega_p\right]$. Now, we can have the expression of $\mathbb{P}(c_p)$ as

$$\mathbb{P}(c_p) = \prod_{i=1}^{n_p} \mathbb{P}(c_p^i) = \pi_p^{c_p^i} \cdot \prod_{i=1}^{n_p-1} \left[\mathsf{F}_p^{\langle c_p^i, c_p^{i+1}\rangle}(\omega_p)\right].$$

Finally, π_p^{t} can be obtained with

$$\pi_p^{\mathrm{t}} = \left\lceil \frac{MTU}{S_p} \right\rceil \cdot \sum_{\text{all } c_p} \pi_p^{c_p^i} \cdot \prod_{i=1}^{\left\lceil \frac{S_p}{MTU} \right\rceil - 1} \left[\mathsf{F}_p^{\langle c_p^i, c_p^{i+1}\rangle}(\omega_p)\right]. \quad (6)$$

The overdue loss rate is dependent on the end-to-end delay. The end-to-end transmission delay (D_p) is dominated by the queueing delay at the bottleneck link and can be approximated by an exponential distribution [16][25]. Thus, the overdue loss rate can be expressed as

$$\pi_p^{\mathrm{o}} = \exp\left[-\frac{\mathrm{T}}{\mathbb{E}\left(D_p\right)}\right], \quad (7)$$

in which $\mathbb{E}(\cdot)$ represents the expectation value. Conventionally, $\mathbb{E}\left(D_p\right)$ needs to be empirically determined from end-to-end delay statistics. In order to derive a general solution for online operation, we construct a model to approximate the average packet delay. We denote the residual bandwidth of p with ν_p. Then, we can have

$$\nu_p = \mu_p - R_p.$$

As the assigned video streaming rate on each path approaches the available bandwidth, the average packet delay typically increases due to network congestion. We use a fractional function to approximate the delay of the allocated sub-flow rate R_p over path p, *i.e.*,

$$\mathbb{E}\left(D_p\right) = \frac{R_p}{\mu_p} + \frac{\rho_p}{\nu_p},$$

in which ρ_p can be interpreted as the available source of communication path p. The value of ρ_p can be estimated from the latest observations of the path status information

$$\rho_p = \frac{\nu_p' \cdot RTT_p}{2}.$$

If ν_p' is equal to the latest observed residual bandwidth of path p, *i.e.*, $\nu_p' = \nu_p$, the one-way delay is $RTT_p/2$. Then, we can have

$$\pi_p^{\mathrm{o}} = \exp\left(-\frac{2 \times \mathrm{T} \cdot \nu_p \cdot \mu_p}{\nu_p' \cdot RTT_p \cdot \mu_p + 2 \times \nu_p \cdot R_p}\right). \quad (8)$$

The effective loss rate can be obtained with Equations (4), (5) and (8).

C. Energy-Distortion Tradeoff

The end-to-end distortion based on the flow rate allocation vector can be expressed as

$$\mathsf{D} = \frac{\alpha}{R - R_0} + \beta \cdot \frac{\sum_{p\in\mathcal{P}} R_p \cdot \Pi_p}{\sum_{p\in\mathcal{P}} R_p}, \quad (9)$$

Therefore, D is proportional to the flow rate allocated to the paths with higher effective loss rate. The effective loss rate represents the communication path quality, and thus is distinct from the packet loss rate, available bandwidth, or round trip time. We have the following proposition to reveal the energy-distortion tradeoff for multihomed video communication over heterogeneous wireless networks:

***Proposition** 1:* For the same video flow allocated over multiple wireless access networks (e.g., Wi-Fi, 3G, LTE), the end-to-end video distortion is inversely proportional to the total energy consumption, i.e., the higher energy consumption results in lower video distortion.

Proof: According to the existing studies [2][17], the cellular networks exhibit better substantiality for user mobility than the Wi-Fi networks. Thus, the effective loss rate of the Wi-Fi network is higher than that of cellular networks, *i.e.*, $\Pi_W > \Pi_C$. On the other side, the energy consumption of delivering the same amount of data using the Wi-Fi interface is lower than that of the cellular network, *i.e.*, $\mathsf{e}_W < \mathsf{e}_C$. Assume there are two rate allocation schemes $a = [R_W^a, R_C^a]$ and $b = [R_W^b, R_C^b]$ for the same video flow of rate R ($R_W^a < R_W^b, R_C^a > R_C^b$). The comparison of energy consumption is as follows.

$$R_W^a \cdot \mathsf{e}_W + R_C^a \cdot \mathsf{e}_C > R_W^b \cdot \mathsf{e}_W + R_C^b \cdot \mathsf{e}_C \Rightarrow \mathbf{E}_a > \mathbf{E}_b.$$

On the other side, the comparison of the end-to-end distortion is as follows

$$\underbrace{\frac{R_W^a \cdot \Pi_W + R_C^a \cdot \Pi_C}{R}}_{\Pi^a} < \underbrace{\frac{R_W^b \cdot \Pi_W + R_C^b \cdot \Pi_C}{R}}_{\Pi^b} \Rightarrow \mathsf{D}^a < \mathsf{D}^b.$$

Therefore, we can arrive at the conclusion that allocating more video traffic data to the cellular network result in higher energy consumption but also achieves better video quality in terms of PSNR. ■

We present the following example to explain the energy-distortion tradeoff in detail.

***Example** 1: Assume a high-definition (HD) video flow of 2.5 Mbps is concurrently transmitted through both Wi-Fi and cellular to the mobile client as shown in Figure 1. Figure 3a shows the evolutions of the power consumption and PSNR per video frame during the interval of $[0, 20]$ seconds. We can observe the variations of the PSNR values for the received video frames track closely to the power consumption. Such results verify the conclusion in Proposition 1. The allocated video data for Wi-Fi and cellular are shown in Figure 3b. It can be observed the power consumption generally enlarges as the Wi-Fi usage increases.*

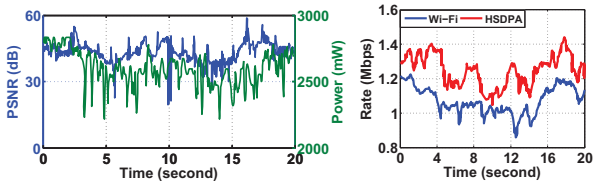

(a) PSNR and power variation (b) rate allocation

Fig. 3. Video flow rate allocation and power consumption over both Wi-Fi and cellular networks.

III. Proposed EDAM Framework

A. Problem Formulation

The optimization problem can be stated as: given the feedback channel status $\{RTT_p, \mu_p, \pi_p^B\}_{p\in\mathcal{P}}$, quality requirement $\overline{\mathsf{D}}$, delay constraint T, and input video frames, find the optimal flow rate allocation vector to minimize the energy consumption. Mathematically, this *distortion constrained energy minimization* problem can be formulated as follows.

$$\textbf{For each flow rate allocation interval, determine the values of } \mathsf{R} = \{R_p\}_{p\in P}$$

$$\textbf{to minimize } \mathbf{E} = \sum_{p\in P} R_p \cdot \mathsf{e}_p, \tag{10}$$

$$\text{subject to } \begin{cases} \sum_{p\in\mathcal{P}} R_p \cdot \Pi_p = \frac{R}{\beta} \cdot \left(\overline{D} - D_0 - \frac{\alpha}{R - R_0}\right), & \text{(11a)} \\ R_p \le \mu_p \cdot (1 - \pi_B), & \text{(11b)} \\ \frac{R_p}{\mu_p} + \frac{\nu_p' \cdot RTT_p}{2 \times \nu_p} \le \mathrm{T}. & \text{(11c)} \end{cases}$$

Constraint 11a states the distortion constraint ($\overline{\mathsf{D}}$) imposed by the video application. The constraints 11b and 11c regulate the capacity and delay constraints for each communication path, respectively. This optimization problem is a precedence constrained multiple knapsack problem and each communication path p considered as a knapsack with properties $\{RTT_p, \mu_p, \pi_p^B\}$. The available items are the sub-flow (R_p), and the profit associate with each sub-flow is the distortion and energy consumption. Such knapsack problem is NP-hard [21] and we present in the next section a heuristic algorithm with polynomial time complexity.

B. Flow Rate Allocation

The solution procedure of the proposed flow rate allocation scheme can be summarized as follows: 1) the calculation of total required video traffic rate to satisfy the imposed quality constraint $\overline{\mathsf{D}}$; 2) multipath data allocation based on utility maximization and piecewise linear approximation.

Traffic Rate Adjustment: The traffic rate adjustment procedure is motivated by Proposition 1, *i.e.*, higher video quality requires more energy consumption. Thus, we present an algorithm to appropriately reduce the traffic rate according to the quality requirement $\overline{\mathsf{D}}$ and video content parameters. Specifically, the video frames are characterized by different priority [*e.g.*, Intra (I), Predicted (P), Bidirectional (B) frames], decoding dependency, *etc*. As the proposed EDAM is a transport-layer protocol and the video encoding parameters are out of the control scope, we propose to selectively drop the frames to reduce the traffic rate under quality constraint.

Note that the removal of higher priority frames (*e.g.*, I frame) can reduce more traffic rate than the lower-weight frames, but this operation will result in the decoding failure of subsequent frames. Algorithm 1 obtains the minimum traffic rate R to satisfy the upper bound of video distortion $\overline{\mathsf{D}}$, by dropping the video frames with lower priority. The authors in [22] prove the loss-free bandwidth ($\mu_p \cdot (1 - \pi_p^B)$) is able to indicate the path quality. Therefore, we assume the initial rate assignment is proportional to this parameter. We assume there totally F frames to be scheduled and each frame $f \in \mathcal{F}$ is associated with a weight w_f. Algorithm 1 summarizes the video traffic rate adjustment procedure.

Algorithm 1: Video traffic rate adjustment

Input: $\{RTT_p, \mu_p, \pi_p\}_{p\in\mathcal{P}}$, T, $\overline{\mathsf{D}}$, R, video frames;
Output: R;
while $D \le \overline{D}$ **do**
  Drop frame $f = \min_{f\in\mathcal{F}}\{w_f\}$ and update traffic rate R;
  $R_p = \frac{\mu_p \cdot (1-\pi_p^B) \cdot R}{\sum_{p\in\mathcal{P}} \mu_p \cdot (1-\pi_p^B)}, \forall p \in \mathcal{P}$;
  $\Pi_p = \pi_p^{\mathrm{t}}(R_p) + \left[1 - \pi_p^{\mathrm{t}}(R_p)\right] \cdot \pi_p^{\mathrm{o}}(R_p)$;
  $\mathsf{D} = \frac{\alpha}{R - R_0} + \beta \cdot \frac{\sum_{p\in\mathcal{P}} R_p \cdot \Pi_p}{\sum_{p\in\mathcal{P}} R_p}$;
end

Rate Allocation Algorithm: As D is dependent on the sum of the transmission and overdue loss rate over each communication path, a piecewise linear approximation can be obtained based on an univariate function. It can be achieved by dividing the interest region of each univariate function into a sufficient number of non-overlapped small intervals. Then, we can approximate the goal function on every hypercube by a convex PWL function. In fact, the goal function **E** corresponds to the arbitrary univariate function $l(\cdot)$ and any potential rate allocation vector is the breakpoint of the PWL function. Therefore, how to find the appropriate breakpoints and judge whether it is an inflection point is the key point for implementing the piecewise approximation of the video rate allocation problem. We seek to solve the multiple knapsack problem by employing the utility maximization theory and the motivation can be summarized as follows.

***Proposition** 2: The utility maximization based on piecewise linear approximation is able to achieve a flow rate allocation vector to approach the minimal energy consumption under quality constraint.*

Proof: The proof is provided in Appendix A. ■

To achieve target video quality, the rate allocation algorithm is inclined to assign loads to the communication paths with higher quality. The quality level offered by a path is proportional to its transmission ability. However, this policy will in turn result in load imbalance and link congestion during the transmission process. Similarly, the energy-minimized allocation may also result in the overload problem by allocating video flows to the communication path with lowest power consumption. In order to alleviate severe load imbalance

problems, we introduce a load imbalance parameter L_p to indicate whether path p is overloaded and it can be expressed as

$$L_p = \frac{\mu_p \cdot (1-\pi_p) - R_p}{\left(\sum_{p\in\mathcal{P}} \mu_p \cdot (1-\pi_p) - \sum_{p\in\mathcal{P}} R_p\right)/P}, \tag{12}$$

in which $\mu_p \cdot (1-\pi_p)$ denotes the 'loss-free' bandwidth of p. When the value of L_p is obviously higher than a threshold limit value (TLV) [19], path p is overloaded. We assume the initial rate allocation for each path is proportional to the available bandwidth, *i.e.*, $R_p = R \cdot \mu_p / \sum_{p\in\mathcal{P}} \mu_p$. Let ΔR_p denote the rate variation over path p at each iteration and $R_p + \Delta R_p$ represent the transition of the next allocation. The utility of this transition can be expressed as [25]:

$$U_p(R_p) = \frac{\varphi\left(R_p + \Delta R_p\right) - \varphi(R_p)}{\Delta R_p}, \tag{13}$$

in which $\varphi(\cdot)$ represents the approximate linear function for D_{total} in the interval $[R_p, R_p + \Delta R_p]$. The utility matrix can be expressed as $\mathcal{U} = \{U_p\}_{p\in\mathcal{P}}$. In each iteration, the proposed flow rate assignment algorithm obtains the R_p that brings the highest utility, *i.e.*,

$$\mathsf{R} = \underset{\{R_p\}_{p\in\mathcal{P}}}{\operatorname{argmax}} \left\{ \sum_{p\in\mathcal{P}} U_p(R_p) \right\}. \tag{14}$$

The proposed algorithm allocates the channel resources available in heterogeneous wireless networks in an iterative manner. Once the resources of path p are exhausted, the algorithm will seek a different path which can release the required resources for the video flow. This operation will be performed until the system utility cannot be improved or the the channel resources available are depleted. The sketch of the flow rate allocation algorithm based utility maximization theory is presented in Algorithm 2.

***Proposition** 3:* The time complexity in the worst case of Algorithm 1 is $O(\frac{P\cdot R}{\Delta R})$, where P denotes the number of available communication paths

Proof: The time complexity of Algorithm 1 is $O(P)$, in which P is the number of available paths. As P is finite integers in practice, the time complexity of Algorithm 1 is acceptable in most cases and is significantly lower compared with the traffic transmission delay. ■

C. Congestion and Retransmission Control

The main purpose of the congestion control in EDAM is to maximize data throughput while respecting TCP-friendliness [10]. Each communication path employs the following parameters: round trip time (RTT_p), congestion window size ($cwnd_p$), slow start threshold ($ssthresh_p$) and retransmission timeout (RTO_p). The ACKs of received packets across all the paths are provided on the aggregate level. The latest aggregate feedback is sent by the destination upon the receipt of each packet. An interesting feature in the congestion control of EDMA is that the ACK packets are sent back through the most reliable uplink communication path to the sender side. This approach mitigates the problem of dropped/overdue feedback packets and increases the measurement accuracy.

Algorithm 2: Flow rate allocation based on utility maximization and piecewise linear approximation

Input: $\{RTT_p, \mu_p, \pi_p\}_{p\in\mathcal{P}}$, T, $TLV = 1.2$, $\Delta R = 0.05 \times R$;
Output: $\mathcal{R} = \{R_p\}_{p\in\mathcal{P}}$;
foreach *path p in* $\mathcal{P}$ **do**
  $R_p \Leftarrow \frac{\mu_p\cdot(1-\pi_p^B)\cdot R}{\sum_{p\in\mathcal{P}} \mu_p\cdot(1-\pi_p^B)}$, $U_p(R_p) \Leftarrow \frac{\varphi\left(R_p+\Delta R_p\right)-\varphi(R_p)}{\Delta R_p}$;
  $L_p \Leftarrow \frac{\mu_p\cdot\left(1-\pi_p\right)-\sum_{f\in\mathcal{F}} R_p}{\left(\sum_{p\in\mathcal{P}} \mu_p\cdot\left(1-\pi_p\right)-\sum_{p\in\mathcal{P}} R_p\right)/P}$;
  while $(L_p \le TLV)\&\&(R_p \le \mu_p\cdot(1-\pi_p^B))$ **do**
    $\Delta R_p \Leftarrow \Delta R_p/U_p$, $R_p \Leftarrow R_p + \Delta R_p$;
    Update the approximate function $\varphi(R_p)$;
  end
end
$\mathsf{R} = \underset{R_p}{\operatorname{argmax}} \left\{\sum_{p\in\mathcal{P}} U_p(R_p)\right\}$;
Improvement for the feasible solution:
if $(L_p \le TLV)\&\&(R_p \le \mu_p\cdot(1-\pi_p^B))$ **then**
  Update free resources of path p;
  find other path p' subject to:
  $(L_{p'} \le TLV)\&\&(R_{p'} \le \mu_{p'}\cdot(1-\pi_{p'}^B))$ ▷ Inter-path allocation;
  if $\Delta U_p > 0$ **then**
    $R_p \Leftarrow R_p - \Delta R_p$, $R_{p'} \Leftarrow R_{p'} + \Delta R_p$;
    Update the available resources of path p and p';
  end
end

The packet loss rates are updated once an ACK is received on any communication path. The round trip time for each communication path is estimated with

$$RTT_p = \begin{cases} \tau_p + \frac{MTU}{\mu_p}, & \text{if } \mu_p\cdot\tau_p \ge cwnd_p, \\ \frac{cwnd_p}{\mu_p}, & \text{otherwise,} \end{cases}$$

in which τ_p denotes the path propagation delay. This latency can be measured based on the timestamps and sequence numbers of consecutive arrival packets [4].

In the environment of heterogeneous access networks, the different physical characteristics or network conditions will result in path asymmetry. The uniform congestion control may induce performance degradation caused by the paths with lower quality. For a specific communication path, the aggregate selective/cumulative ACK feedback is filtered to obtain the delivery status of the scheduled packets. The per-path ACK information is used for sliding the congestion window of the path. A timer called retransmission timeout (RTO_p) is set while delivering new data to path p and RTO_p is obtained with

$$RTO_p = RTT_p + 4 \times \sigma_{RTT_p}.$$

The response to a timeout is identical to the conventional TCP. EDAM does not perform fast retransmissions since it may result in unnecessary transmissions. The slow start threshold ($ssthresh_p$) will be set to $\max(cwnd_p/2, 4\times MTU)$ after receiving four duplicated selective acknowledgements.

The adaption rules that regulate the multipath congestion control in EDAM to achieve TCP-friendliness are stated in the following proposition.

***Proposition** 4:* Let $\mathbf{I}(cwnd_p)$ and $\mathbf{D}(cwnd_p)$ denote the increasing and decreasing functions of the congestion window size for path p, respectively. The sufficient and necessary condition to achieve TCP-friendly congestion control is $\mathbf{I}(cwnd_p) = \frac{3\times\mathbf{D}(cwnd_p)}{2-\mathbf{D}(cwnd_p)}$.

Proof: The proof is provided in Appendix B. ■

In the emulations of this work, we set the congestion window adaption functions as follows.

$$\mathbf{I}(cwnd_p)=\frac{3\times\beta}{2\times\sqrt{cwnd_p+1}-\beta}, \mathbf{D}(cwnd_p)=\frac{\beta}{\sqrt{cwnd_p+1}},$$

in which $\beta \in \{0.1, 0.2, ..., 0.9\}$. Note that the value of β for the AIMD algorithm in TCP is 0.5.

The delay constraint and energy consumption are seldom considered in existing MPTCP retransmission schemes. To reduce the unnecessary retransmissions for conserving bandwidth and energy, this paper proposes a delay and energy aware retransmission control scheme. Specifically, the lost packet will be retransmitted through the lowest energy-consumed path that could deliver the packet within the deadline. The packet loss differentiation is based on the average RTT ($\overline{RTT}_p$), standard deviation (σ_{RTT}), and number of consecutive losses (l_p) [23].

Algorithm 3: Congestion and retransmission control

$\overline{RTT} \Leftarrow (31/32) \times \overline{RTT} + (1/32) \times RTT$;
$\sigma_{RTT} \Leftarrow (15/16) \times \sigma_{RTT} + (1/16) \times |RTT - \overline{RTT}|$;
Cond_I $\Leftarrow (l_p == 1)$ && $(RTT_p < \overline{RTT}_p - \sigma_{RTT_p})$;
Cond_II $\Leftarrow (l_p == 2)$ && $(RTT_p < \overline{RTT}_p - \sigma_{RTT_p}/2)$;
Cond_III $\Leftarrow (l_p == 3)$ && $(RTT_p < \overline{RTT}_p)$;
Cond_IV $\Leftarrow (l_p > 3)$ && $(RTT_p < \overline{RTT}_p - \sigma_{RTT_p}/2)$;
if *packet loss occurs over communication path* p **then**
  if Cond_I||Cond_II||Cond_III||Cond_IV $== true$ **then**
    $ssthresh_p = \max(cwnd_p/2, 4 \times MTU)$;
    $cwnd_p = MTU$;
  end
  if *received* 4 *duplicated SACK* **then**
    $ssthresh_p = \max(cwnd_p/2, 4 \times MTU)$;
    $cwnd_p = ssthresh_p$;
  end
  $\mathcal{P}' = \mathcal{P} \cap \{p \in \mathbb{E}\{D_p\} < \mathrm{T}\}$;
  $p_{\min} = \arg\min_{p\in\mathcal{P}'} \{\mathsf{e}_p\}$;
  Retransmit the lost packet through $p_{\min}$;
end

IV. Performance Evaluation

In this section, we evaluate the performance of the proposed EDAM through extensive semi-physical emulations in Exata. First, we describe the evaluation methodology that includes the emulation setup, performance metrics, reference schemes, and emulation scenario. Then, we depict and discuss the evaluation results in detail.

A. Evaluation Methodology

Emulation Setup: We adopt the Exata and JM as the network emulator and video codec, respectively. The architecture of the performance evaluation system is presented in Figure 4 and the main configurations are set as follows.

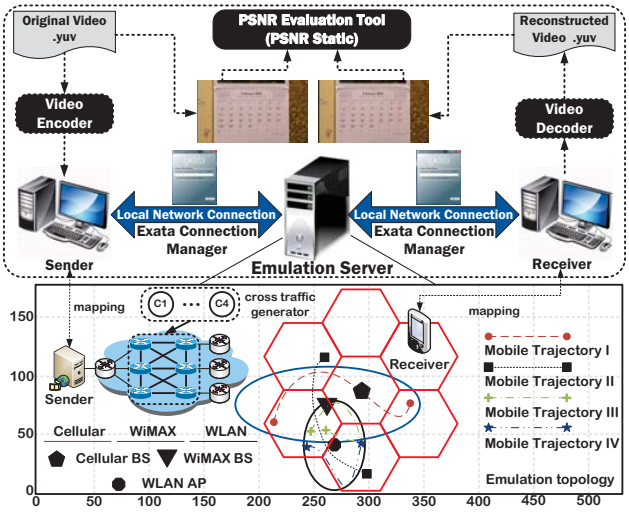

Fig. 4. System architecture and network topology for performance evaluation.

Network Emulator: Exata 2.1 [18] is used as the network emulator. Exata is an advanced edition of QualNet [26] in which we can perform semi-physical emulations. In order to implement the real-video-streaming based emulations, we integrate the source code of JM with Exata and develop an application layer protocol of "Video Transmission". The detailed descriptions of the development steps could be referred to Exata Programmer's Guide [18]. In the emulated network topology, the sender has one wired network interface and the mobile client has three wireless network interfaces, *i.e.*, Cellular, WLAN and WiMAX. The parameter configurations of different wireless networks are summarized in Table I. As the Exata emulator does not include MPTCP in the transport-layer stacks, we develop this transport protocol based on the TCP module and the C code (of MPTCP Linux implementation) from GitHub [19]. As depicted in the figure, each router is attached to one edge node, which is single-homed and introduces background traffic. Each of the edge nodes has four traffic generators producing cross traffic with a Pareto distribution. The packet sizes of background traffic are varied to mimic the real traces collected on the Internet: 50% of them are 44-Byte long, 25% have 576 Bytes, and 25% are 1500-Byte long. The aggregate cross traffic loads imposed on the available network paths are similar and vary randomly between $20-40$ percent of the bottleneck links' bandwidth. The data distribution interval is 250 ms (the duration of a GoP) and the TLV is 1.2 [25]. The packet interleaving level (ω_p) is 5 ms for each path.

Video Codec: H.264/AVC reference software JM 18.2 [20] is adopted as the video encoder. The generated video streaming is encoded at 30 frames per second and a GoP consists of 15 frames. The GoP structure is IPPP. The test video sequences are *blue sky, mobcal, park joy, and river bed* in high definition (HD) content. These test sequences feature different patterns of temporal motion and spatial characteristics that reflected in their corresponding video quality versus encoding rates. We concatenate the video sequences to be 6000

TABLE I
CONFIGURATIONS OF WIRELESS NETWORKS

Cellular parameter	Value
Common control channel power	33 dB
Maximum power of BS	43 dB
Total cell bandwidth	3.84 Mb/s
Target SIR value	10 dB
Orthogonality factor	0.4
Inter/intra cell interference ratio	0.55
Background noise power	-106 dB
$\mu_p, \pi^B, 1/\xi^B$	1500 Kbps, 2%, 10 ms
WiMAX parameter	**Value**
System bandwidth	7 MHz
Number of carriers	256
Sampling factor	8/7
Average SNR	15 dB
Symbol duration	2048
$\mu_p, \pi^B, 1/\xi^B$	1200 Kbps, 4%, 15 ms
WLAN parameter	**Value**
Average channel bit rate	8 Mbps
Slot time	10 μs
Maximum contention window	32
$\mu_p, \pi^B, 1/\xi^B$	1000 Kbps, 6%, 12 ms

frame-long in order to obtain statistically meaningful results. The tolerable loss rate (Δ) and delay constraint (T) are set to be 1% and 250 ms, respectively. The streaming video is encoded at the source rates of 2.4, 2.2, 2.8, and 1.85 Mbps for the Trajectory I to IV. The available capacities are just enough or very tight for delivering the encoded video streaming.

Performance Metrics:

- Energy and power consumption. The energy consumption is expressed in units of Joule (J) and the power consumption value is presented in mW. These evaluation results are estimated using the energy model in Exata [18].
- PSNR. PSNR (Peak Signal-to-Noise Ratio) is the standard metric of objective video quality and is a function of the MSE between the original and the received video frames. If a video frame either experiences transmission or overdue loss, it is considered to be dropped and will be concealed by copying from the last received frame.
- Inter-packet delay. We measure the inter-packet delay of received packets to quantify the jitter of delivered video stream. High jitter values between packets cause bad visual quality (*e.g.*, video glitches and stalls during the display).

Reference Schemes:

- EMTCP [4]. The energy-efficient MPTCP scheme leverages the throughput-energy tradeoff for the path selection and congestion control. We use the algorithm for real-time applications proposed in [4] for comparison.
- MPTCP [10]. The baseline MPTCP scheme is used as a reference. The congestion control, path selection and data retransmission mechanisms can be referred to the MPTCP development guideline [10].

Emulation Scenarios: We conduct the semi-physical emulations in mobile scenarios and the trajectories are shown in Figure 4. To evaluate the performance in energy saving, we set the target quality at 25, 31 and 37 dB for all the competing schemes along different trajectories. Similarly, the comparison of video quality are based on the same level of energy consumption. To obtain the average results with 95% confidence interval, each emulation is performed more than 10 times. The microscopic results are the data refined from a single run with the least noise interference.

B. Evaluation Results

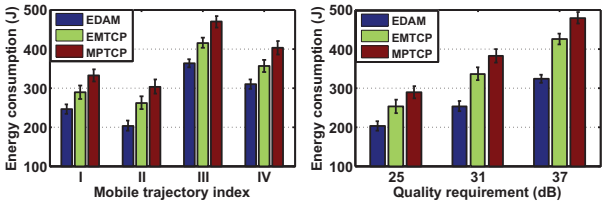

(a) different trajectories (b) different requirements

Fig. 5. Comparison of energy consumption.

Energy Consumption: The average energy consumption values for the competing schemes along different trajectories are shown in Figure 5a. The proposed EDAM achieves the lowest energy consumption level in all the mobile emulation scenarios. EDAM outperforms the EMTCP as we consider the distortion rather than the throughput in the flow rate allocation. Due to the special future of video streaming, a higher throughput cannot always guarantee better video quality. For instance, allocating video data to a communication path with available bandwidth but high propagation delay will increase the throughput but further degrade the video quality. This is because the sub-flow dispatched onto this path will experience deadline violations. Figure 5b illustrates the energy consumption for different quality requirements along the Trajectory I. It can be observed the superiority of EDAM over the reference schemes becomes more obvious as the quality requirement increases. The results' trend also verify the tradeoff between video quality and energy consumption for the same video flow over heterogeneous access networks.

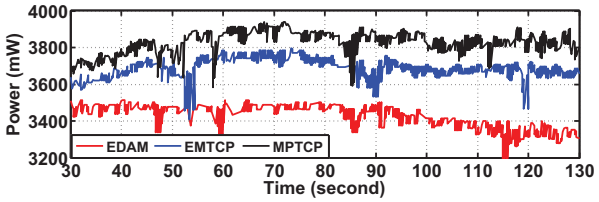

Fig. 6. Comparison of power consumption during the interval of $[30, 130]$ seconds.

Figure 6 shows the power consumption of the competing schemes during the interval of $[30, 130]$ seconds. The results are obtained with the throughput of all the access networks. EDAM achieves lower power consumptions and variations during the multipath video communication.

PSNR: We gradually decrease the distortion constraint ($\overline{\mathrm{D}}$) of the proposed EDAM to achieve the same energy consumption level as the reference schemes. The resulting average PSNR results in different mobile trajectories are shown in Figure 7a and we can see the results' pattern is almost the

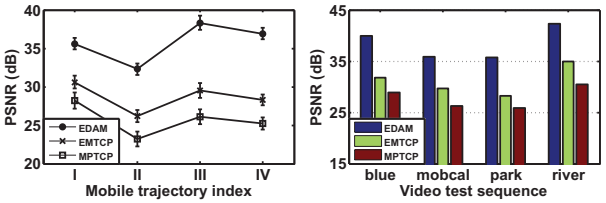

(a) different trajectories (b) different sequences

Fig. 7. Comparison of average PSNR results.

same as shown in Figure 5a. It is also in accordance with the Proposition 1, *i.e.*, higher energy consumption generally results in higher video quality. EDAM outperforms the reference schemes and the performance gaps become larger in Trajectory III. It indicates the superiority of EDAM in overcoming the path diversity in heterogeneous access networks and integrating the available bandwidth. Figure 7b shows the average PSNR values for different video test sequences.

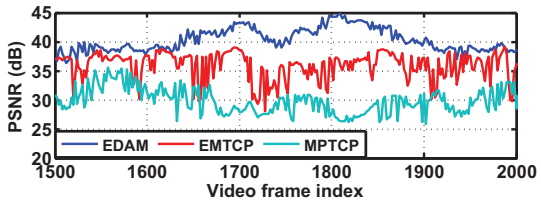

Fig. 8. Comparison of PSNR per video frame indexed from 1500 to 2000.

To compare the microscopic quality results, we plot the instantaneous PSNR values (measured from the *blue sky* sequence) for the video frames indexed from 1500 to 2000 in Figure 8. EDAM achieves higher values with lower variations to guarantee the excellent perceived quality (above 37 dB) while the reference schemes frequently induce violations of imposed distortion constraint.

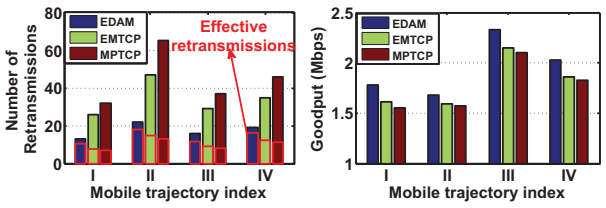

(a) retransmissions (b) average goodput

Fig. 9. Comparison of retransmission and goodput performance.

Retransmissions: In Figure 9a, we plot the number of total and effective retransmissions of all the MPTCP schemes. EDAM achieves higher ratio of effective retransmissions with smaller number of total retransmissions as it takes into account the delay constraint of video applications. Furthermore, the retransmissions performed by EDAM are through the low energy-consumption path that guarantees in-time delivery. A higher number of effective retransmissions also increases the goodput values shown as in Figure 9b.

V. Conclusion and Discussion

The ever-growing popularity of powerful mobile terminals enables individual users to access the Internet and watch videos from everywhere. MPTCP is the standard transport-layer protocol to enable multipath data transfer in multihomed communication environments. In this paper, we propose a novel Energy-Distortion Aware MPTCP (EDAM) scheme to enable the energy efficient and quality guaranteed video streaming over heterogeneous wireless networks. Through modeling and analysis, we develop solutions for the flow rate allocation and data retransmission control. Experimental results show that EDAM outperforms the existing MPTCP schemes in reducing the energy consumption and improving the video quality (in terms of PSNR). As future work, we will improve the congestion control and send buffer management algorithms in EDAM to further improve video data throughput.

Appendix A: Proof for Proposition 2

Let $l(\cdot)$ denote an univariate function with the interest region of $[a, a'] \subset \mathbb{R}$. We assume z breakpoints in the region are appropriately chosen so that $l(\cdot)$ can be approached by the function $\hat{l}(r) = \mathrm{A}_r \cdot x + \mathrm{B}_r$ in each small interval $I_r = [a_{r-1}, a_r]$, $1 \le r \le z+1$. A_r and B_r are determined by the linear equations $l(a_{r-1}) = \hat{l}(a_{r-1})$ and $l(a_r) = \hat{l}(a_r)$. The approximation function $\varphi(\cdot)$ of $l(\cdot)$ on $[a, a']$ can be obtained via connecting these intervals.

For any r in the interval of $(1, z)$, we name a_r an turning point if $\mathrm{A}_r > \mathrm{A}_{r+1}$. Let $a_{t(1)} < \ldots < a_{t(q)}$ denote all the turning points among the breakpoints $[a_1, a_z]$. We define $\hat{I}_t = [a_{t(i-1)}, a_{t(i)}], a \le i \le q+1$. It can be observed that $\hat{I}_t$ is the union of intervals $I_r, t(i-1) < r < t(i)$. Based on the aforementioned partition, we can obtain a piecewise-convex expression of the function $\varphi(\cdot)$, which is very useful to obtain the global optimization of separable programming problems. Then, we can have for any $i \in [1, q+1]$

$$\varphi(\eta) = \max_{r \in \{t(i-1), t(i)\}} \left\{ \hat{l}_r(\eta) \right\}, \forall\, \eta \in \hat{I}_t.$$

We use the proof by contradiction to obtain the above equation. The relationships $\mathrm{A}_{t(i-1)+1} < \mathrm{A}_{t(i-1)+2} < \ldots < \mathrm{A}_{t(i)}$ are true in the interval of $1 \le i \le q+1$. Then, the function $\varphi(\cdot)$ is convex on $\hat{I}_t$ for any $\hat{\eta} \in \hat{I}_t$. There is an integer $r \in \hat{s}_t$ to satisfy $\hat{\eta} \in I_r$ and $\varphi(\hat{\eta}) = \hat{l}_r(\hat{\eta})$. Then, we can obtain the following inequality

$$\hat{l}_{r'}(\hat{\eta}) \le \hat{l}_r(\hat{\eta}),\ t(i-1) < r' < t(i)\ \&\&\ r' \ne r. \qquad (15)$$

Or else, there exists the r' $(t(i-1) < r' < t(i)\ \&\&\ r' \ne r)$ to satisfy $\hat{l}_{r'}(\hat{\eta}) > \hat{l}_r(\hat{\eta})$. Then, we can choose $\bar{\eta} \in \hat{I}_{r'} \subset \hat{I}_t$ and a small positive number ϖ so that the equation $\eta' = \varpi \cdot \hat{\eta} + (1-\varpi) \cdot \bar{\eta}$ $(\bar{\eta} \in I_{r'})$ can be obtained. As the approximation function $\varphi(\cdot)$ is convex in the interval of $\hat{I}_t$, we can have

$$\begin{aligned} \varphi(\eta') &\le \varpi \cdot \varphi(\hat{\eta}) + (1-\varpi) \cdot \varphi(\bar{\eta}), \\ &= \varpi \cdot \hat{l}_r(\hat{\eta}) + (1-\varpi) \cdot \hat{l}_r(\bar{\eta}), \\ &< \varpi \cdot \hat{l}_{k'}(\hat{\eta}) + (1-\varpi) \cdot \hat{l}_{r'}(\bar{\eta}) = \hat{l}_{r'}(\eta'). \end{aligned}$$

The above result contradicts the $\varphi(\eta') = \hat{l}_{r'}(\eta')$. As the value of λ' is randomly chosen, we can prove Equation (15) is true.

Hence, we can approach the goal function on every hypercube by a convex piecewise linear function.

APPENDIX B: PROOF FOR PROPOSITION 4

Assume there are two video flows sharing the same bottleneck link, delivered using the proposed EDAM and TCP respectively. We use the notations $cwnd_p$ and $cwnd'_p$ to denote the congestion window sizes of the congestion control mechanism in EDAM and AIMD algorithm in TCP. In the normal state (*i.e.*, the bottleneck link is underloaded), the evolutions of the congestion windows during the interval of $[t, t+\Delta t]$ are as follows.

$$cwnd_p(t+\Delta t) = cwnd_p(t) + \mathbf{I}(cwnd_p)\cdot\Delta t,$$
$$cwnd'_p(t+\Delta t) = cwnd'_p(t) + \Delta t.$$

In the case of link congestion occurs (we assume the video application using TCP is also able to identify the congestion loss), both the video flows decrease the congestion window sizes following the equations of

$$\begin{cases} cwnd_p(t_i) + cwnd'_p(t_i) = cwnd_{\max}, \\ cwnd_p(t_{i+1}) = cwnd_p(t_i)\cdot[1-\mathbf{D}(cwnd_p)], \\ cwnd'_p(t_{i+1}) = \frac{1}{2}\cdot cwnd'(t_i). \end{cases}$$

The time interval between t_i and t_{i+1} is the decision epoch. Therefore, we can obtain

$$cwnd_p(t_{i+1}) - cwnd_p(t_i) = \frac{cwnd_{\max}\cdot\mathbf{I}(cwnd_p) - [2\times\mathbf{D}(cwnd_p)\cdot cwnd_p(t_i) + \mathbf{I}(cwnd_p)]\cdot cwnd_p(t_i)}{2\times[\mathbf{I}(cwnd_p)+1]}.$$

After a sufficient number of scheduling cycles, the congestion window sizes of the two competing flows will converge to

$$cwnd_p(t_\infty) = \frac{cwnd_{\max}\cdot\mathbf{I}(cwnd_p)}{\mathbf{I}(cwnd_p) + 2\times\mathbf{D}(cwnd_p)},$$
$$cwnd'_p(t_\infty) = \frac{2\times cwnd_{\max}\cdot\mathbf{D}(cwnd_p)}{\mathbf{I}(cwnd_p) + 2\times\mathbf{D}(cwnd_p)}.$$

Therefore, the values of $cwnd_p$ and $cwnd'_p$ increase and decrease periodically in the long run. The average values can be approached with

$$\overline{cwnd}_p = \frac{cwnd_{\max}\cdot[2-\mathbf{D}(cwnd_p)]\cdot\mathbf{I}(cwnd_p)}{2\times\mathbf{I}(cwnd_p) + 4\times\mathbf{D}(cwnd_p)},$$
$$\overline{cwnd}'_p = \frac{3\times cwnd_{\max}\cdot\mathbf{D}(cwnd_p)}{2\times\mathbf{I}(cwnd_p) + 4\times\mathbf{D}(cwnd_p)}.$$

To guarantee the fairness in bandwidth sharing, the congestion window size of EDAM should be equal to that of the TCP, *i.e.*,

$$\overline{cwnd}_p = \overline{cwnd}'_p \Rightarrow \mathbf{I}(cwnd_p) = \frac{3\times\mathbf{D}(cwnd_p)}{2-\mathbf{D}(cwnd_p)}.$$

REFERENCES

[1] http://galaxys5guide.com/samsung-galaxy-s5-features-explained/galaxy-s5-download-booster/

[2] S. Deng, R. Netravali, A. Sivaraman, et al., "WiFi, LTE, or Both?: measuring multi-homed wireless internet performance," in *Proc. of ACM IMC*, 2014.

[3] Cisco, "Visual Networking Index: Global Mobile Data Traffic Forecast Update, 2014-2019," Feb. 2015.

[4] Q. Peng, M. Chen, et al., "Energy-Efficient Multipath TCP for Mobile Devices," in *Proc. of ACM MobiHoc*, 2014.

[5] D. Wischik, C. Raiciu, A. Greenhalgh, et al., "Design, Implementation and Evaluation of Congestion Control for Multipath TCP," in *Proc. of USENIX NSDI*, 2011.

[6] Y. C. Chen, Y. Lim, R. J. Gibbens, et al., "A Measurement-based Study of Multipath TCP Performance over Wireless Networks," in *Proc. of ACM IMC*, 2013.

[7] M. A. Hoque, M. Siekkinen, J. K. Nurminen, "Using crowd-sourced viewing statistics to save energy in wireless video streaming, in *Proc. of ACM MobiCom*, 2013.

[8] M. A. Hoque, M. Siekkinen, et al., "Energy efficient multimedia streaming to mobile devicesła survey," *IEEE Commun. Surv. Tutor.*, vol. 16, no. 1, pp. 579-597, 2014.

[9] J. Wu, C. Yuen, B. Cheng, M. Wang, J. Chen, "Energy-Minimized Multipath Video Transport to Mobile Devices in Heterogeneous Wireless Networks," *IEEE J. Sel. Areas Commun.*, to be published, DOI: 10.1109/JSAC.2016.2551483.

[10] A. Ford, C. Raiciu, et al., "Architectural guidelines for multipath TCP development," IETF RFC 6182, 2011.

[11] C. Raiciu, C. Paasch, S. Barre, et al., "How Hard Can It Be? Designing and Implementing a Deployable Multipath TCP," in *Proc. of USENIX NSDI*, 2012.

[12] R. Khalili, N. Gast, M. Popovic, et al., "MPTCP is not pareto-optimal: performance issues and a possible solution," in *Proc. of ACM CoNEXT*, 2012.

[13] E. Gilbert, "Capacity of a burst-noise channel," *Bell Syst. Tech. J.*, vol. 39, no. 9, pp. 1253-1265, 1960.

[14] K. Stuhlmüller, N. Färber, et al., "Analysis of video transmission over lossy channels," *IEEE J. Sel. Areas Commun.*, vol. 18, no. 6, pp. 1012-1032, 2000.

[15] E. Harjula, O. Kassinen, M. Ylianttila, "Energy consumption model for mobile devices in 3G and WLAN networks," in *Proc. of IEEE CCNC*, 2012.

[16] L. Zhou, X. Wang, et al., "Distributed scheduling scheme for video streaming over multi-channel multi-radio multi-hop wireless networks," *IEEE J. Sel. Area Commun.*, vol. 28, no. 3, pp. 409-419, 2010.

[17] T. Oliveira, S. Mahadevan, D. P. Agrawal, "Handling network uncertainty in heterogeneous wireless networks," in *Proc. of IEEE INFOCOM*, 2011.

[18] Exata homepage. http://www.scalable-networks.com/

[19] https://github.com/multipath-tcp/mptcp/

[20] http://iphome.hhi.de/suehring/tml/

[21] S. Martello,"Heuristic algorithms for the multiple knapsack problem," Computing, vol. 27, no. 2, pp. 93-112, 1981.

[22] V. Sharma, K. Kar, et al., "A transport protocol to exploit multipath diversity in wireless networks," *IEEE/ACM Trans. Netw.*, vol. 20, no. 4, pp. 1024-1039, 2012.

[23] S. Cen, P. C. Cosman, G. M. Voelker, "End-to-end differentiation of congestion and wireless losses," *IEEE/ACM Trans. Netw.*, vol. 11, no. 5, pp. 703-717, 2003.

[24] J. Wu, C. Yuen, B. Cheng, M. Wang, J. Chen, "Streaming High-Quality Mobile Video with Multipath TCP in Heterogeneous Wireless Networks," *IEEE Trans. Mobile Comput.*, to be published, DOI: 10.1109/TMC.2015.2497238.

[25] J. Wu, B. Cheng, C. Yuen, Y. Shang, J. Chen, "Distortion-Aware Concurrent Multipath Transfer for Mobile Video Streaming in Heterogeneous Wireless Networks," *IEEE Trans. Mobile Comput.*, vol. 14, no. 4, pp.688-701, 2015.

[26] QualNet homepage. www.scalable-networks.com/qualnet

[27] Y. Cui, L. Wang, X. Wang, H. Wang, Y. Wang, "FMTCP: A fountain code-based multipath transmission control protocol," in *Proc. of IEEE ICDCS*, 2012.